Adaptive Underwater Image Enhancement Guided by Generalized Imaging Components

Yonghua Tang, Xu Liu, *Student Member, IEEE*, Zhipeng Zhang, and Sen Lin, *Member, IEEE*

***Abstract*—Underwater images often exhibit strong color distortion and hazing due to various degradation factors. A majority of algorithms provide color correction for underwater images, but the color is not as vivid as it could be. In order to solve this problem, we propose a method known as adaptive underwater image enhancement guided by generalized imaging components (AUIE-GIC). To the best of our knowledge, this is the first method of utilizing deep learning to develop a generalized imaging model. The proposed method contains two stages: component generation and component guided learning. In the first stage, we obtain the components of a learning-based generalized imaging model. In the second stage, attenuation and transmission features are used to adjust color and semantic information. We propose the attenuation attention module (AAM), and transmission attention module (TAM), which can highlight heavily degraded areas. Finally, the refined network is able to restore underwater images that are rich in semantics and vivid in color. Based on further evaluation and analysis, AUIE-GIC is demonstrated to provide superior performance when compared with state-of-the-art (SOTA) methods.**

***Index Terms*—Generalized imaging model, adaptive learning, underwater image enhancement.**

I. Introduction

THE processing and analysis of underwater images plays an important role in communication, navigation, and precision operations for underwater vehicles [1], [2], [3]. Yet, underwater images are often subjected to strong degradation [4]. Water absorbs more light as wavelengths increase, and it is most easily absorbed by the red and yellow light. As a result, underwater images are usually green or blue in color. In addition, underwater images often have severe hazing. Compared to land images, underwater images are more degraded, and the reasons are complicated, making it difficult to obtain clear images directly. Consequently, a proposal for an efficient and effective underwater image enhancement algorithm is of great research value.

The current underwater image enhancement can be roughly divided into three categories: **model-free methods**; **model-based methods** and **learning-based methods**. For model-free methods [5], [6], [7], It is only necessary to modify the pixel values of an image, such as the histogram equalization (HE) algorithms, the white balance (WB) algorithms, and the transform domain filtering (TDF) algorithms. In model-based approaches [8], [9], degraded images are mathematically modelled. Common models include underwater optical imaging model (UOIM), underwater retinex model (URM), etc. As computing devices have been upgraded, learning-based methods [10], [11], [12], [13], [14], [15], [16], [17], [18] have gradually become more prevalent. In contrast to traditional algorithms, deep neural networks achieve better results by learning end-to-end from degraded images to clear images without resorting to any prior knowledge.

However, traditional approaches (model-free/traditional model-based methods) may be accompanied by noise, strong exposure, or other decorative effects. Yuan et al. [6] employ contour bougie morphology to enhance underwater images and add several operations to the outline. However, noise will be introduced to images and the enhanced result has obvious color cast and overexposure. A restoration algorithm is proposed by Wang et al. [19] that is based on an adaptive attenuation-curve prior and can provide a more accurate estimation of the underwater optical imaging model. The image generated by this method has red artifacts. Deep learning methods often lack texture details, are not vividly colored, and have visible haze. Peng et al. [20] propose the U-shape transformer for deep underwater image enhancement, which removes color artifacts and casts. Li et al. [13] complete the enhancement task through a network with multiple color spaces, as well as using transmission maps to assist in network learning. But the processed image still has severe haze. A novel underwater image enhancement framework is presented in this article to address these problems:

- ▶*Orientation:* We propose a method namely adaptive underwater image enhancement guided by generalized imaging components (AUIE-GIC). To our best knowledge, it is the first method to develop a learnable underwater generalized imaging model (LUGIM). It can be divided into two stages. In the first stage, we decompose the input image by LUGIM. The second stage of network learning is guided in an adaptive manner by using partial imaging components.
- ▶*Bringing Color Back to Life:* Images taken underwater tend to be blue-green in color. The attenuation term in the generalized model can reflect the color representation. We proposed the attenuation attention module (AAM), which assigns weights

Manuscript received 27 August 2023; revised 12 November 2023; accepted 13 November 2023. Date of publication 24 November 2023; date of current version 6 December 2023. This work was supported by the Applied Basic Research Program of Liaoning Province under Grant 2023JH2/101300237. The associate editor coordinating the review of this manuscript and approving it for publication was Dr. Yu Liu. *(Corresponding author: Xu Liu.)*

Yonghua Tang and Zhipeng Zhang are with the School of Information Science and Engineering, Shenyang University of Technology, Shenyang 110870, China (e-mail: 229286824@qq.com; 1159328074@qq.com).

Xu Liu is with the School of Computer Science and Information Engineering, Hefei University of Technology, Hefei 230601, China (e-mail: dalong.xu.liu@ieee.org).

Sen Lin is with the School of Automation and Electrical Engineering, Shenyang Ligong University, Shenyang 110159, China (e-mail: lin_sen6@126.com).

We make the source code available at https://github.com/perseveranceLX/AUIE-GIC.

Digital Object Identifier 10.1109/LSP.2023.3336578

according to degrees of color degradation. Therefore, the color processing is more sensitive and generated images are more attractive and lively.

- ▶*Bringing Semantic Information Back to Life:* Hazing in underwater images is a significant problem, resulting in a lack of semantic information. In the generalized model, the transmission contain semantic information. A transmission attention module (TAM) allows the network to allocate different weight to different regions. Thus, it can more efficiently learn from clear images, make enhancement results brighter without hazing.

Based on comprehensive experiments, the proposed method is capable of effectively enhancing underwater images, ensuring better colors and reducing hazing.

II. Methodology

In this section, we will provide a comprehensive description of the proposed algorithm. First, we propose a learnable underwater generalized imaging model (LUGIM). Then, we refine the images by adaptive guidence of imaging components. As a result of these two stages, a clear and visually appealing underwater image is obtained.

A. Learnable Imaging Model

Since the attenuation of forward scattered light is much smaller than that of direct reflected light, forward scattering has a minimal effect on imaging quality. As a consequence, underwater optical imaging model (UOIM) is typically represented as a sum of direct component and background light component:

$$\mathcal{I}(x) = \underbrace{\mathcal{J}(x)\cdot\mathcal{T}(x)}_{\text{Direct Component}} + \underbrace{\mathcal{A}(x)\cdot(1-\mathcal{T}(x))}_{\text{Background Light Component}} \tag{1}$$

where $\mathcal{I}(x)$ is the degraded underwater image, $\mathcal{J}(x)$ means the clear image, $\mathcal{T}(x)$ represents the transmission map and the $\mathcal{A}(x)$ is the background light. Moreover, an underwater environment can also benefit from the underwater retinex model (URM). Degraded image $\mathcal{I}(x)$ is composed of illumination $\mathcal{L}(x)$ and reflection $\mathcal{R}(x)$ results:

$$\mathcal{I}(x) = \mathcal{L}(x)\cdot\mathcal{R}(x) \tag{2}$$

where $\mathcal{L}$(x) and $\mathcal{R}$(x) are the illumination component and the reflectance component, respectively. While UOIM eliminates the impact of the light source, affecting the color of the restored image. The URM does not consider background light, which may result in poor image visual quality. Inspired by the generalized imaging model (GIM) for dehazing [21], we developed a LUGIM for enhancing underwater images as follows:

$$\begin{aligned}
&\mathcal{I}(x) = (\mathcal{J}(x)\cdot\mathcal{T}(x) + \mathcal{A}(x)\cdot(1-\mathcal{T}(x)))\cdot\mathcal{C}(x),\\
&\mathcal{J}(x) = \mathcal{G}_J(\mathcal{I}(x)), \mathcal{T}(x) = \mathcal{G}_T(\mathcal{I}(x)),\\
&\mathcal{A}(x) = \mathcal{G}_A(\mathcal{I}(x)), \mathcal{C}(x) = \mathcal{G}_C(\mathcal{I}(x)).
\end{aligned} \tag{3}$$

where $\mathcal{C}(x)$ is the attenuation which contains the color representation, $\mathcal{G}_J$, $\mathcal{G}_T$, $\mathcal{G}_A$ and $\mathcal{G}_C$ are four network (J-Net, T-Net, A-Net and C-Net) that estimate these components respectively. With $\mathcal{C}(x)$ and $\mathcal{T}(x)$, the network can be guided appropriately for color correction and dehazing.

B. Adaptive Learning by Components Guidance

According to LUGIM, we get the $\mathcal{J}$(x) component that represents a clear image. However, we find that the visual result of $\mathcal{J}$(x) is not acceptable, as shown in Fig. 2. To obtain better results, we propose two attention modules, namely an attenuation attention module (AAM) and a transmission attention module (TAM) for learning degradation distribution. And a refine-net for dynamic enhancement through these two guides. Given the color representation $\mathcal{C}(x)$ and the input degraded image $\mathcal{I}(x)$, the goal of AAM is to learn the channel attention map $\mathcal{E}_\mathcal{C}(x)$:

$$\mathcal{W}_\mathcal{C}(x) = \mathcal{H}_\mathcal{C}(\mathcal{C}(x)), \mathcal{E}_\mathcal{C}(x) = \mathcal{W}_\mathcal{C}(x)\cdot\mathcal{I}(x). \tag{4}$$

where $\mathcal{W}_\mathcal{C}(x) \in \mathbb{R}^{3\times1\times1}$ is the channel weight, $\mathcal{H}_\mathcal{C}$ means the attenuation attention generator.

The $\mathcal{T}(x)$ contains semantic information. As a further step towards obtaining a distribution of semantic information degradation, we employ TAM to learn the channel and pixel attention map $\mathcal{E}_\mathcal{T}(x)$ (since $\mathcal{E}_\mathcal{C}(x)$ represents the channel attention map, $\mathcal{E}_\mathcal{T}(x)$ can be seen as multiplying pixel weights on $\mathcal{E}_\mathcal{C}(x)$, so it is called channel and pixel attention map):

$$\mathcal{W}_\mathcal{T}(x) = \mathcal{H}_\mathcal{T}(\mathcal{T}(x)), \mathcal{E}_\mathcal{T}(x) = \mathcal{W}_\mathcal{T}(x)\cdot\mathcal{E}_\mathcal{C}(x). \tag{5}$$

where $\mathcal{W}_\mathcal{T}(x) \in \mathbb{R}^{1\times h\times w}$ is the pixel weight, $\mathcal{H}_\mathcal{T}$ means the transmission attention generator. As well as describing the degradation distribution of color, $\mathcal{W}_\mathcal{T}(x)$ also contains the degradation distribution of semantic information. Fig. 3. shows the details of two attention weight generators: $\mathcal{H}_\mathcal{C}$ and $\mathcal{H}_\mathcal{T}$.

Through these two modules, the network integrates the color information of different channels and semantic information under different pixels, and focuses on processing severely degraded channels and pixels through Refine-Net:

$$\begin{aligned}
\mathcal{O}(x) &= \mathcal{R}(\mathcal{M}(x)),\\
\mathcal{M}(x) &= \mathcal{E}_\mathcal{T}(x) + \mathcal{I}(x),
\end{aligned} \tag{6}$$

where $\mathcal{M}(x)$ represent the Refine-Net, $\mathcal{M}(x)$ is the result of residual connection.

C. Loss Function

The algorithm proposed in this article is mainly achieved through asynchronous learning, which includes two stages: the establishment of LUGIM and the refinement of the final results. We combine the WMSE loss ($\mathcal{L}_{\text{WMSE}}$) [17], L1 loss ($\mathcal{L}_1$) and VGG loss ($\mathcal{L}_{\text{VGG}}$) [22] for two stages:

$$\begin{cases}
\mathcal{L}^{\text{I}} = \mathcal{L}^{\text{a}}_{\text{I}} + \mathcal{L}^{\text{b}}_{\text{I}},\\
\mathcal{L}^{\text{a}}_{\text{I}} = \mathcal{L}_{\text{WMSE}}(\mathcal{I}_{\text{Rec}}, \mathcal{I}) + \mathcal{L}_{\text{WMSE}}(\mathcal{J}, \mathcal{J}_{\text{GT}}),\\
\mathcal{L}^{b}_{\text{I}} = \mathcal{L}_1(\mathcal{I}_{\text{Rec}}, \mathcal{I}) + \mathcal{L}_1(\mathcal{J}, \mathcal{J}_{\text{GT}})\\
\qquad +\lambda\cdot(\mathcal{L}_{\text{VGG}}(\mathcal{I}_{\text{Rec}}, \mathcal{I}) + \mathcal{L}_{\text{VGG}}(\mathcal{J}, \mathcal{J}_{\text{GT}})),\\
\mathcal{I}_{\text{Rec}} = (\mathcal{J}\cdot\mathcal{T} + \mathcal{B}\cdot(1-\mathcal{T}))\cdot\mathcal{C}.
\end{cases} \tag{7}$$

$$\begin{cases}
\mathcal{L}^{\text{II}} = \mathcal{L}^{\text{a}}_{\text{II}} + \mathcal{L}^{\text{b}}_{\text{II}},\\
\mathcal{L}^{\text{a}}_{\text{II}} = \mathcal{L}_{\text{WMSE}}(\mathcal{O}, \mathcal{O}_{\text{GT}}),\\
\mathcal{L}^{b}_{\text{II}} = \mathcal{L}_1(\mathcal{O}, \mathcal{O}_{\text{GT}}) + \lambda\cdot\mathcal{L}_{\text{VGG}}(\mathcal{O}, \mathcal{O}_{\text{GT}})).
\end{cases} \tag{8}$$

where $\mathcal{L}^{\text{I}}$ and $\mathcal{L}^{\text{II}}$ are losses of the stage I and the stage II respectively, $\mathcal{J}_{\text{GT}}$ and $\mathcal{O}_{\text{GT}}$ all mean the ground truth of datasets.

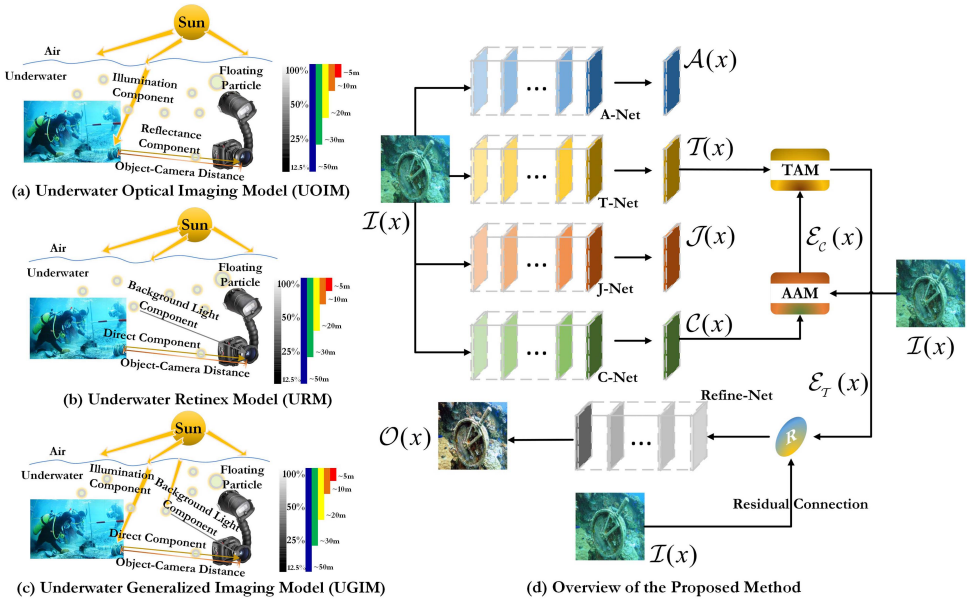

Fig. 1. Demonstration of the underwater optical imaging model (UOIM), the underwater retinex model (URM), the underwater generalized imaging model (UGIM) and our proposed method.

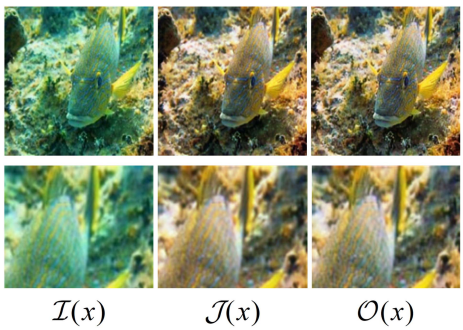

Fig. 2. Why not to use $\mathcal{J}(x)$? Through the LUGIM, we obtain four components of the degraded image: $\mathcal{J}(x)$; $\mathcal{T}(x)$; $\mathcal{B}(x)$ and $\mathcal{C}(x)$, where $\mathcal{J}(x)$ represents the clear image in LUGIM. $\mathcal{O}(x)$ is the final result by adaptive correction of AAM, TAM and refine-net. The generated $\mathcal{J}(x)$ correct the overall color and remove haze, the colors in local areas are not vivid, and lack some semantic information.

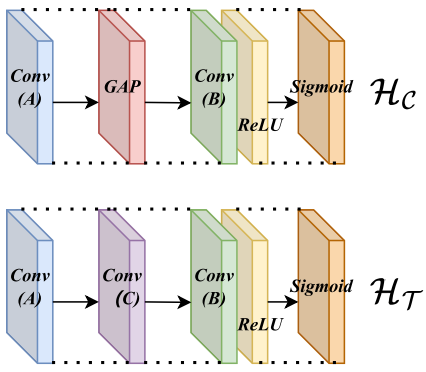

Fig. 3. Details of the $\mathcal{H}_{\mathcal{C}}$ and the $\mathcal{H}_{\mathcal{T}}$. Conv (A) and Conv (C) are 3×3 and 1×1 convolutional layers. Conv (B) is the 3×3 separable convolutional layer. GAP represents the global adaptive pooling. ReLU and Sigmoid mean activation functions.

III. Experiments

A. Implementation Details

Following the Boths [17], we use the same training and testing conditions. Also, the Boths is the backbone of our proposed method (A-Net, T-Net, J-Net, C-net and Refine-Net). For the purpose of evaluating the enhanced results between the AUIE-GIC and state-of-the-art (SOTA) models, we use eight deep learning-based methods: GAN-RS [10], WaterNet [11], FUnIE-GAN [12], Ucolor [13], LCNet [14], UICoENet [15], LANet [16], Boths [17], and three prior-driven methods: MAMF [5], ACS [6], TEBCF [7].

B. Objective and Subjective Evaluation

In this subsection, we will process an comprehensive evaluation of our proposed method. For the objective evaluation, we use five metrics: MSE; RMSE; PSNR; SSIM and LPIPS [23], which are measure the distance between the enhanced result and the ground truth. The results are shown in Table I. For the subjective evaluation, we make the visual comparison of these 12 methods (including our proposed AUIE-GIC) in Fig. 4. It is obvious that our proposed method has advantages in various image evaluation indicators. The enhanced image is closer to the ground truth, clearer and brighter, and has less noise, which can effectively solve problems such as hazing and color cast.

C. Ablation Study

In this section, we indicate the effect of every component proposed in this network. We train and test four baselines ($\mathcal{J}(x)$, w/o AAM, w/o TAM, full method). The $\mathcal{J}(x)$ is the result of the first stage (LUGIM). The w/o AAM and w/o TAM mean full method without AAM or TAM. The visual results and

TABLE I
THE OBJECTIVE EVALUATION OF AUIE-GIC AND STATE-OF-THE-ART (SOTA) METHODS

Full-reference		Methods												
		Raw	MAMF	ACS	TEBCF	GAN-RS	Water-Net	FUnIE-GAN	Ucolor	LCNet	UICoE-Net	LANet	Boths	*AUIE-GIC*
UVE-38K	MSE ↓	478.7659	+640.6002	-44.4484	+24.4249	+265.5804	-209.4494	-86.7205	-253.3041	-134.2906	-184.5762	-54.2780	-262.4129	**-340.6266**
	RMSE ↓	21.8807	+11.5762	-1.0404	+0.5512	+5.4020	-5.4699	-2.0806	-6.8653	-3.3207	-4.7288	-1.2776	-7.1718	**-10.1275**
	PSNR ↑	23.1592	-5.1997	-1.2171	-1.7739	-2.7070	+2.5536	+0.5800	+2.6805	+0.4629	+1.0176	+0.3348	+4.4747	**+5.2607**
	SSIM ↑	0.8826	-0.0677	-0.0383	-0.0788	-0.0909	+0.0361	-0.0075	+0.0348	+0.0243	+0.0362	+0.0248	+0.0404	**+0.0579**
	LPIPS ↓	0.2700	+0.0430	-0.0182	+0.0105	+0.0174	-0.1124	+0.0138	-0.1244	-0.0493	-0.1038	-0.1119	-0.1425	**0.1670**
EUVP	MSE ↓	105.6025	+801.6708	+540.1754	+552.1642	+1115.5923	+158.7409	+49.6593	+256.6242	+143.9673	+192.2217	+362.8863	+49.6885	**+27.4332**
	RMSE ↓	10.2763	+19.8488	+15.1359	+15.3707	+24.6693	+5.9823	+2.1841	+8.7560	+5.5215	+6.9813	+11.3683	+2.1853	**+1.2578**
	PSNR ↑	28.9184	-9.5767	-8.2490	-8.3908	-10.9628	-3.2728	-1.3924	-5.2044	-4.2018	-4.9450	-6.2509	-1.2592	**-0.5151**
	SSIM ↑	0.8883	-0.1251	-0.0981	-0.1025	-0.1635	-0.0047	-0.0163	-0.0077	-0.0248	-0.0175	-0.0271	+0.0048	**+0.0104**
	LPIPS ↓	0.3047	+0.1743	+0.0489	+0.0414	+0.0767	-0.0250	**-0.1046**	-0.0295	+0.0204	-0.0215	-0.0178	-0.0490	-0.0793
UIEB	MSE ↓	744.7855	+227.9463	-171.9322	-160.7421	+19.3221	-327.8433	-196.3625	-501.8527	-145.9688	-392.3290	-492.0680	-487.6904	**-568.9413**
	RMSE ↓	27.2908	+3.8979	-3.3564	-3.1238	+0.3517	-6.8716	-3.8723	-11.7045	-2.8200	-8.5169	-11.3937	-11.2566	**-14.0302**
	PSNR ↑	21.3411	-1.7709	+0.1142	-0.0186	-1.3805	+2.4826	+1.1942	+4.5068	+0.8270	+3.4878	+4.4609	+4.3378	**+6.1477**
	SSIM ↑	0.8187	-0.0005	+0.0204	+0.0238	-0.0408	+0.0579	+0.0394	+0.0765	+0.0485	**+0.1018**	+0.0867	+0.0859	+0.0910
	LPIPS ↓	0.2771	+0.1109	+0.0025	-0.0242	+0.0332	-0.1092	+0.0303	-0.1336	-0.0332	-0.1122	-0.1374	+0.1281	**+0.1413**

In this case, we use the metrics values of the raw image as the standard, with +/- representing the offset between its metrics values and the metrics values of other methods.
The best values are indicated in bold.

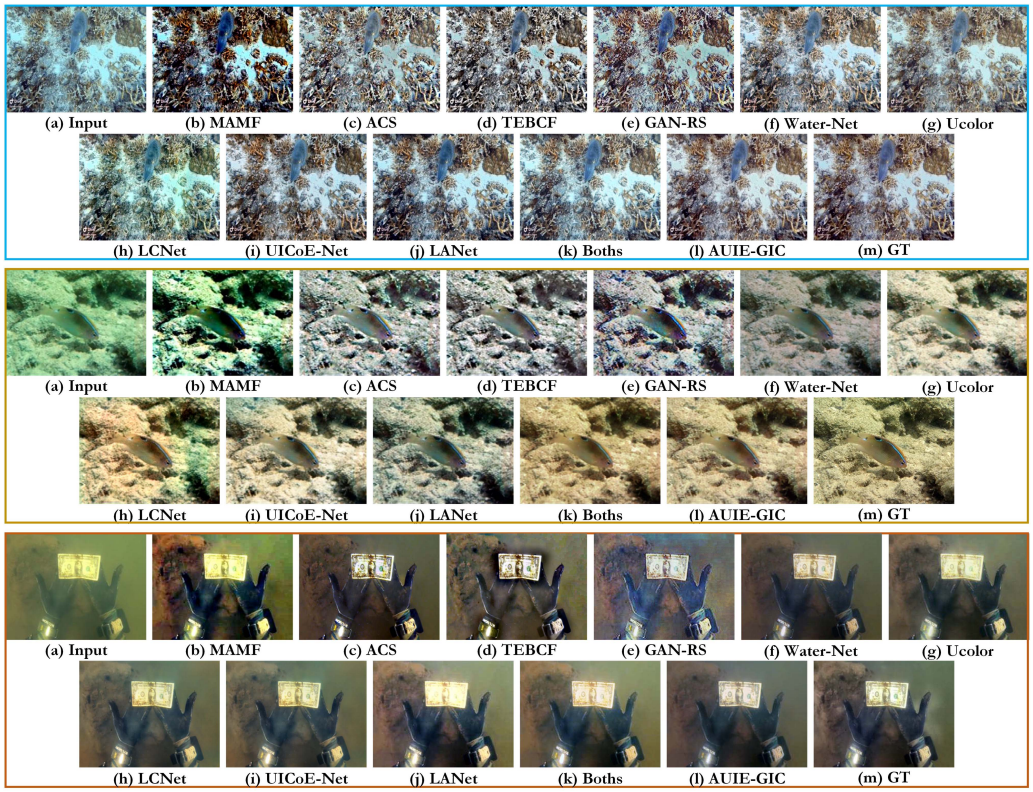

Fig. 4. Subjective evaluation of our proposed AUIE-GIC and state-of-the-art (SOTA) methods. GT is the ground truth.

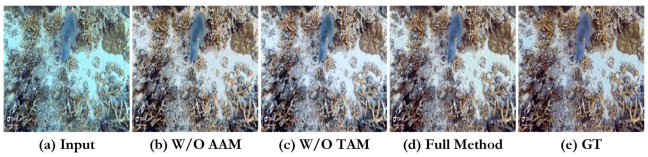

Fig. 5. Subjective evaluation of the ablation study.

TABLE II
OBJECTIVE EVALUATION OF THE ABLATION STUDY

Ablation study	Baselines			
	$\mathcal{J}(x)$	W/O AAM	W/O TAM	*Full Method*
PSNR ↑	27.7742	27.9355	28.1030	**28.4199**
SSIM ↑	0.9283	0.9309	0.9343	**0.9405**
LPIPS ↓	0.1237	0.1223	0.1102	**0.1030**

The best values are indicated in bold.

quantitative results are shown in Fig. 5 and Table II respectively. Fig. 2. presents a detailed comparison between $\mathcal{J}(x)$ and $\mathcal{O}(x)$. Thus, it will not be compared here again. Through visual and metric results, it can be clearly seen that w/o AAM makes local colors no longer lifelike, and w/o TAM lacks details. Furthermore, it proves that all the modules proposed in this article are effective.

IV. CONCLUSION

This article proposes a novel underwater image enhancement network called AUIE-GIC, which is the first attempt to drive underwater generalized imaging models through deep learning. There are two stages in the proposed method: component generation and adaptive learning. In numerous subjective and objective studies, AUI-GIC has been demonstrated to be capable of resolving color and semantic information with exceptional efficiency.

REFERENCES

[1] E. Ashford, T. L. Flanagan, N. Ashford, and E. Ashford, "Championing the future of ghost pot recovery through the implementation of remotely operated vehicles and community science models," in *Proc. OCEANS San Diego–Porto*, 2021, pp. 1–4.

[2] Z. Gong, C. Li, and F. Jiang, "AUV-Aided joint localization and time synchronization for underwater acoustic sensor networks," *IEEE Signal Process. Lett.*, vol. 25, no. 4, pp. 477–481, Apr. 2018, doi: 10.1109/LSP.2018.2799699.

[3] B. Wang and X. Guan, "Channel estimation for underwater acoustic communications based on orthogonal chirp division multiplexing," *IEEE Signal Process. Lett.*, vol. 28, pp. 1883–1887, 2021, doi: 10.1109/LSP.2021.3111569.

[4] C. Li, J. Guo, and C. Guo, "Emerging from water: Underwater image color correction based on weakly supervised color transfer," *IEEE Signal Process. Lett.*, vol. 25, no. 3, pp. 323–327, Mar. 2018, doi: 10.1109/LSP.2018.2792050.

[5] Y. Cho, J. Jeong, and A. Kim, "Model-assisted multiband fusion for single image enhancement and applications to robot vision," *IEEE Robot. Autom. Lett.*, vol. 3, no. 4, pp. 2822–2829, Oct. 2018.

[6] J. Yuan, W. Cao, Z. Cai, and B. Su, "An underwater image vision enhancement algorithm based on contour bougie morphology," *IEEE Trans. Geosci. Remote Sens.*, vol. 59, no. 10, pp. 8117–8128, Oct. 2021.

[7] J. Yuan, Z. Cai, and W. Cao, "TEBCF: Real-world underwater image texture enhancement model based on blurriness and color fusion," *IEEE Trans. Geosci. Remote Sens.*, vol. 60, 2022, Art. no. 4204315.

[8] Z. Liang, X. Ding, Y. Wang, X. Yan, and X. Fu, "GUDCP: Generalization of underwater dark channel prior for underwater image restoration," *IEEE Trans. Circuits Syst. Video Technol.*, vol. 32, no. 7, pp. 4879–4884, Jul. 2022.

[9] S. Lin et al., "Underwater image sharpening based on structure restoration and texture enhancement," *Appl. Opt.*, vol. 60, no. 15, pp. 4443–4454, 2021.

[10] X. Chen, J. Yu, S. Kong, Z. Wu, X. Fang, and L. Wen, "Towards real-time advancement of underwater visual quality with GAN," *IEEE Trans. Ind. Electron.*, vol. 66, no. 12, pp. 9350–9359, Dec. 2019.

[11] C. Li et al., "An underwater image enhancement benchmark dataset and beyond," *IEEE Trans. Image Process.*, vol. 29, pp. 4376–4389, 2020.

[12] M. J. Islam, Y. Xia, and J. Sattar, "Fast underwater image enhancement for improved visual perception," *IEEE Robot. Autom.*, vol. 5, no. 2, pp. 3227–3234, Apr. 2020.

[13] C. Li, S. Anwar, J. Hou, R. Cong, C. Guo, and W. Ren, "Underwater image enhancement via medium transmission-guided multi-color space embedding," *IEEE Trans. Image Process.*, vol. 30, pp. 4985–5000, 2021.

[14] N. Jiang, W. Chen, Y. Lin, T. Zhao, and C.-W. Lin, "Underwater image enhancement with lightweight cascaded network," *IEEE Trans. Multimedia*, vol. 24, pp. 4301–4313, 2022, doi: 10.1109/TMM.2021.3115442.

[15] Q. Qi et al., "Underwater image co-enhancement with correlation feature matching and joint learning," *IEEE Trans. Circuits Syst. Video Technol.*, vol. 32, no. 3, pp. 1133–1147, Mar. 2022.

[16] S. Liu, H. Fan, S. Lin, Q. Wang, N. Ding, and Y. Tang, "Adaptive learning attention network for underwater image enhancement," *IEEE Robot. Autom.*, vol. 7, no. 2, pp. 5326–5333, Apr. 2022.

[17] X. Liu, S. Lin, K. Chi, Z. Tao, and Y. Zhao, "Boths: Super lightweight network-enabled underwater image enhancement," *IEEE Geosci. Remote Sens. Lett.*, vol. 20, 2022, Art. no. 1500405.

[18] X. Liu, S. Lin, and Z. Tao, "Learning multiscale pipeline gated fusion for underwater image enhancement," *Multimedia Tools Appl.*, vol. 82, pp. 1–24, 2023.

[19] Y. Wang, H. Liu, and L. -P. Chau, "Single underwater image restoration using adaptive attenuation-curve prior," *IEEE Trans. Circuits Syst. I: Regular Papers*, vol. 65, no. 3, pp. 992–1002, Mar. 2018, doi: 10.1109/TCSI.2017.2751671.

[20] L. Peng, C. Zhu, and L. Bian, "U-shape transformer for underwater image enhancement," *IEEE Trans. Image Process.*, vol. 32, pp. 3066–3079, 2023, doi: 10.1109/TIP.2023.3276332.

[21] Z. Liang, W. Zhang, R. Ruan, P. Zhuang, and C. Li, "GIFM: An image restoration method with generalized image formation model for poor visible conditions," *IEEE Trans. Geosci. Remote Sens.*, vol. 60, pp. 2022, Art. no. 4110616.

[22] K. Simonyan and A. Zisserman, "Very deep convolutional networks for large-scale image recognition," 2014, arXiv1409.1556.

[23] R. Zhang, P. Isola, A. A. Efros, E. Shechtman, and O. Wang, "The unreasonable effectiveness of deep features as a perceptual metric," in *Proc. IEEE/CVF Conf. Comput. Vis. Pattern Recognit.*, 2018, pp. 586–595.